Eur. Phys. J. A **13**, 27–32 (2002)

THE EUROPEAN PHYSICAL JOURNAL A

Perspectives of few-body approaches to dripline nuclei

M.V. Zhukov[1]
(with RNBT Collaboration)

Department of Physics, Chalmers University of Technology and Göteborg University, S-412 96 Göteborg, Sweden

Received: 1 May 2001

Abstract. Present days' nuclear physics has focused on exploring fundamental nuclear matter under extreme conditions, which can be created in modern accelerator laboratories. The opportunities offered by beams of exotic nuclei for a research in the areas of nuclear-structure physics, nucleosynthesis and nuclear astrophysics are exciting, and the large worldwide activity in the construction of radioactive-beam facilities reflects the strong scientific interest in the physics that can be probed with such beams. On the neutron-rich side of stability radioactive beams have already led to the discovery of halos in nuclei with nucleonic distributions extending to large distances. Light nuclei constitute so far the part of the nuclear landscape where the neutron dripline has been reached. Subsequent developments have deepened and enriched the picture of halos as a pure quantum mechanics phenomenon, where particles can be found far from each other in classically forbidden regions. Few-body dynamics plays a crucial role in every adequate description of the discovered halo properties and just few-body methods lead at the early stage to self-consistent explanations of most of the experimental findings in halo physics. We discuss experiments that probe a halo structure through studying different reactions with halo nuclei. We discuss also theoretical methods and models based on few-body approaches, which allow to extract an accurate spectroscopic information from experiments and make predictions for future experiments.

PACS. 25.60.-t Reactions induced by unstable nuclei – 21.45.+v Few-body systems

1 Introduction

Current nuclear physics has focused on exploring fundamental nuclear matter under extreme conditions, which can be created in modern accelerator laboratories. The large worldwide activity in the construction of radioactive-beam facilities demonstrates the strong scientific interest in the physics that can be probed with beams of exotic nuclei. These beams provide exciting opportunities for a research in the areas of nuclear-structure physics, nucleosynthesis and nuclear astrophysics. The study of unstable (but still stable against particle decay) nuclei embraces many new aspects of nucleonic matter. It focuses on exotic properties of loosely bound quantum systems, often with new geometries, such as nuclei with giant halos or skins of neutron matter with extremely low density. With access to exotic nuclei the very limits of nuclear existence, that is, the edges of the nuclear landscape can be fully explored.

The structural features of the nuclei near driplines change compared to nuclei closer to the beta-stability line. Recent examples are the disappearance of the normal nuclear-shell closures and the introduction of new magic numbers. This is demonstrated by the observations of the breakdown of the $N = 8$ shell closure for ^{12}Be [1,2] and the new magic number $N = 16$ [3].

Light nuclei constitute so far the part of the nuclear landscape where the neutron dripline has been reached. Triggered by the discovery [4] of abnormally spatially extended nuclei (^{6}He, ^{11}Li, ^{11}Be) at the vicinity of the neutron dripline, the initial idea of (binary) halos was suggested in [5]. A nuclear halo state is a threshold phenomenon with extreme clusterization into an ordinary core nucleus and veil of halo nucleons. Since then, the halo phenomenon has been studied very intensively, both experimentally and theoretically, and it is now a well-known structural feature of many light dripline nuclei [6–8]. Few-body dynamics plays a crucial role in every adequate description of the discovered halo properties and just few-body methods lead at the early stage to self-consistent explanations of most of the experimental findings in halo physics such as large sizes, narrow momentum distributions of fragmentation products and huge Coulomb dissociation cross-sections.

In this paper we discuss experiments that probe a halo structure through studying different reactions with halo nuclei. We discuss also theoretical methods and models based on few-body approaches, which allow to extract an accurate spectroscopic information from experiments and make predictions for future experiments. Recent achievements, challenges and perspectives of few-body dynamics in modern halo physics will also be discussed.

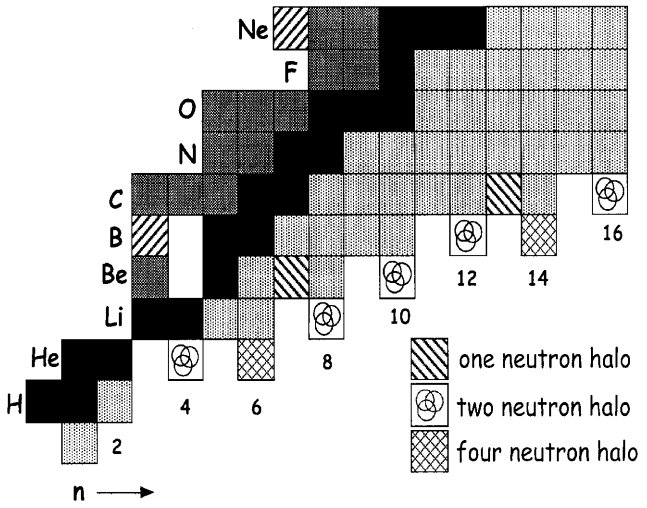

Fig. 1. The lower part of the nuclear chart.

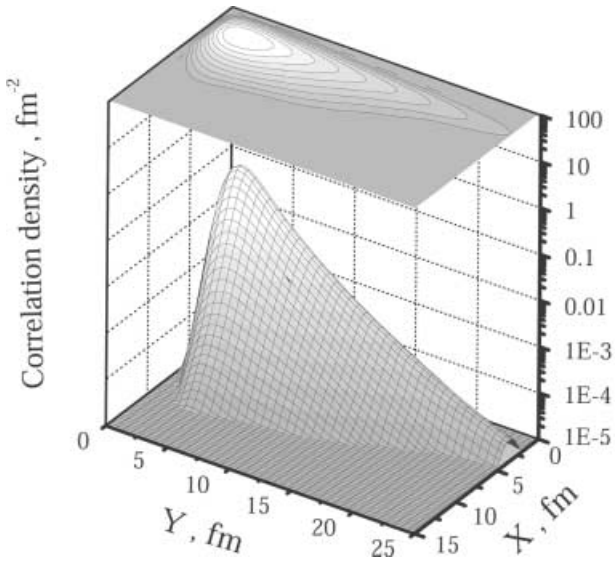

Fig. 2. Correlation density for ^{8}B. X is the relative ^{4}He-^{3}He distance and Y is the distance between a valence proton and the CM of ^{7}Be (the ^{4}He-^{3}He subsystem).

2 Experimental and theoretical studies of halo nuclei

To start the discussion we show in fig. 1 the lower part of the nuclear chart where light nuclei are situated and where both (the proton and the neutron) driplines are well known. Some interesting features are seen in this figure. First of all only a relatively small number of nuclei, shown in black, are stable. The rest of nuclei decay. The closer the nucleus to the dripline, the shorter the lifetime of the nucleus is. This short lifetime prevents, in general, the production of targets from nuclei for investigations of their properties by most of the traditional nuclear-physics methods. That is why little was known about the structure of nuclei in the vicinity of driplines. The beams of radioactive nuclei, which are now available at leading facilities in the world, have changed the situation drastically and have allowed intensive experimental studies of dripline nuclei.

There is another property which is also easily seen in fig. 1. If one starts from a stable nucleus and tries to add more and more neutrons (one by one) then, sooner or later, one comes to the situation when the system cannot keep the last neutron. Still if one adds one more neutron, the system becomes bound once again. Such nuclei (with small separation energy of the last two neutrons) are shown by a special Borromean symbol [6] in fig. 1. They have very peculiar properties and can be considered as genuinely new three-body nuclear systems (a tightly bound core plus two valence neutrons), where other intrinsic degrees of freedom are essentially unimportant. Sometimes such a system is able to keep two more neutrons (but not one), leading to the very neutron-rich systems like ^{8}He and ^{19}B. There are two more interesting nuclei at the neutron-rich side of the nuclear chart (fig. 1). These are ^{11}Be and ^{19}C nuclei which can be considered as two-body nuclear systems (a core plus a valence neutron). Modern experiments show that all these systems possess a neutron halo in their ground states. At the proton-rich side of the nuclear chart (fig. 1) there are at least two nuclei which have to be mentioned. The first one is ^{8}B, which plays a very important role in our understanding of the nucleosynthesis and the solar boron neutrino problem. Recent experimental and theoretical studies of ^{8}B [9,10] allow to speculate about a proton halo in ^{8}B. Figure 2 shows the correlation density for ^{8}B, calculated as a three-body system (^{4}He-^{3}He-p) in [10]. The long tail of the valence proton distribution is clearly seen in fig. 2. The second nucleus is ^{17}Ne which has the Borromean property and which might be considered as a candidate for two-proton halo or a skin [11].

The first experiments with radioactive-beams measured the interaction cross-sections or reaction cross-sections for light neutron dripline nuclei [4]. These experiments revealed abnormally large cross-sections for some light neutron-rich nuclei and provided important information on the nuclear sizes. The data demonstrated a large increase of the radii for ^{6}He, ^{11}Li, ^{11}Be, ^{14}Be, ^{17}B compared to the corresponding previous particle-stable isotopes. Later theoretical studies [12,13] indicated that the sizes of some of these systems can be larger than the ones extracted from the first experiments. For example, the ^{11}Li radius can be as large as 3.55 fm [12] making ^{11}Li comparable in size with stable nuclei having approximately four times more nucleons. This finding can be understood as follows [5,6]: the low separation energy (0.3 MeV) of two valence neutrons combined with the short-range nuclear forces, allow them to tunnel out into the classically forbidden space outside the nuclear core (^{9}Li). This means that two valence neutrons approximately decouple from the core, and have a large spacial extension. So, a veil of a very dilute neutron matter is thus surrounding the core, and creates a halo.

2.1 One-neutron halo nuclei

As shown in [14] two-body nuclear halos are essentially limited to weakly bound neutron-core systems in relative s or p states. The known examples are in the region

where the first s and p states appear at the dripline with small energies. As we have already mentioned the ^{11}Be nucleus is the best-known case of a one-neutron halo nucleus which has the ground-state angular momentum and parity $J^\pi = 1/2^+$. It has the excited $(1/2^-)$ bound state which can be a halo state. It should be noted that quantum numbers $J^\pi = 1/2^+$ of the ^{11}Be ground state contradict the expectations $J^\pi = 1/2^-$ from the traditional shell model. This is an important fact, which shows that we have to deal with an intruder state coming down from the s-d shell. The ground state of another one-neutron halo nucleus ^{19}C has presumably quantum numbers $1/2^+$ [15]. These states are simple illustrations both of the halo structure and the coupling to more complicated states. The ^{10}Be core has an excited 2^+ state which by coupling to the single-particle $0d_{5/2}$ state produces a significant component $\sim 16\%$ (determined from the analysis of a (p,d) reaction with a ^{11}Be beam [16] and from the recent measurement of the ^{11}Be nuclear magnetic moment [17]) in addition to the single-particle $1s_{1/2}$ state coupled to the ground state of ^{10}Be, which is the main component of the ground state of ^{11}Be. This coupling can be responsible for the inversion of s and p states in ^{11}Be [18].

The ^{18}C core has also an excited 2^+ state. Two different states of ^{19}C can then be constructed, *i.e.* one precisely, as for ^{11}Be, resulting in $1/2^+$ and another $5/2^+$ state by coherently adding a single-particle $0d_{5/2}$ state coupled to the ^{18}C core ground state and the $5/2^+$ state resulting from coupling of the 2^+ excited state and the $1s_{1/2}$ state. These two different structures are rather similar as they both contain $1s_{1/2}$ and $0d_{5/2}$ single-particle components. The potentially pronounced halo structures are reduced due to the $0d_{5/2}$ contribution [19]. Their energy sequence is not established although some evidence points to $1/2^+$ as the ground state [15].

Recently new experiments, measuring longitudinal momentum distributions of the heavy fragment (the ^{10}Be-core) from the one-neutron removal channel for ^{11}Be projectile, have been performed. The γ-rays from de-excitation of the heavy fragment were also measured in coincidence with the fragment [20]. This allows to separate and to evaluate the contributions of core fragments in various excited states and to extract momentum distributions which correspond to the neutron removal from individual core states. These data provided important spectroscopic information about this halo nucleus. The theoretical analysis [20–22] of the experimental data on the reaction $^9\mathrm{Be}(^{11}\mathrm{Be}, ^{10}\mathrm{Be}+\gamma)$ with 60 MeV/N ^{11}Be beam is consistent with the experimental finding [20] that about 22% of the one-neutron removal cross-section corresponds to the production of ^{10}Be in low-lying excited states.

There is one more candidate for one-neutron halo among light nuclei, namely $^{15}\mathrm{C}(1/2^+)$, which has a one-neutron separation energy of 1.2 MeV, a narrow core (^{14}C) momentum distribution and a large ($\sim$0.88) spectroscopic factor for the $s_{1/2}$ neutron coupled to the ground state of the $^{14}\mathrm{C}(0^+)$ core. This nucleus is under active investigation now [19,22–24].

2.2 Two-neutron halo nuclei

The two-neutron halo nuclei have received most attention among the halo systems. This is connected with their Borromean character [6], where the three-body system is bound and its all binary subsystems are unbound. It should be mentioned that all known light two-neutron halo nuclei have this property (see fig. 1). The most studied Borromean systems are ^{6}He, ^{11}Li and ^{14}Be. As it was mentioned the essential part of the experimental information about the structure of these nuclei has been obtained through studies of the reactions induced by halo projectiles with targets consisting of stable nuclei.

The largest breakup cross-sections for light targets are related to one neutron and the core in the final state [25, 26]. This is a reason why the neutron and the core momentum distributions were investigated at the first stage both experimentally and theoretically. One can expect that in the simplest approximation, the transparent limit of the Glauber model, these momentum distributions are connected with the Fourier transform of the initial three-body wave function [27]. It appeared, however, that the Fourier transform of the three-body wave function gave larger momentum widths compared with experimental widths. Two important lessons have been learnt from studies of momentum widths. The sizes of all particles (including the target) are important and this effect leads to smaller widths [28,29]. The final-state interaction between the projectile fragments is also very important and it makes the widths narrower [30–32]. During the last decade, few-body theoretical methods for calculations of reactions with two-neutron halo nuclei, have been developed [33–36]. These methods are able to reproduce well, not only the fragment momentum distributions, but also the experimental cross-sections (including heavy targets [35,36], where the Coulomb interaction is very important).

During the last few years new experiments on three-body halo systems were performed. In these experiments the core and one of the halo neutrons (or both neutrons) from breakup reactions were detected in coincidence. These experiments allow to extract correlation observables which give the insight to the internal structure of the halo and allow a comparison with theoretical predictions.

The technique of intensity interferometry was used in [37] to probe the spatial configuration of the Borromean three-body halo nuclei. The n-n momentum distribution from the dissociation of the two-neutron halo nuclei ^{6}He, ^{11}Li and ^{14}Be on a carbon target at incident energies 30–50 MeV/N, were measured and the corresponding n-n correlation functions were extracted (see, fig. 3 taken from [37]). The r_0-values were obtained (see the inserts in fig. 3). These values are connected by a simple formula with r.m.s. n-n separations in the Borromean halo nuclei $r_{\mathrm{nn}}^{\mathrm{rms}} = \sqrt{6}r_0$. As a result, the $r_{\mathrm{nn}}^{\mathrm{rms}} = 5.9 \pm 1.2$, 6.6 ± 1.5 and 5.4 ± 1.0 fm were obtained for three Borromean nuclei ^{6}He, ^{11}Li and ^{14}Be, respectively. These results are in agreement with those predicted from three-body models [6,27,38].

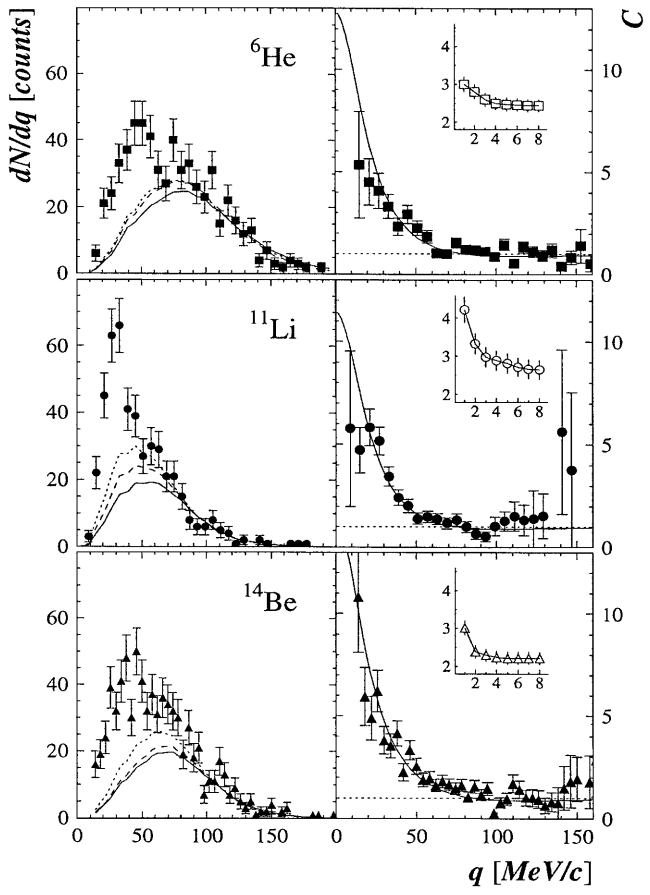

Fig. 3. Correlation functions (right-hand panels) constructed for the three nuclei. The solid lines correspond to the fit using a Gaussian source. On the left, the measured n-n momentum distributions (symbols) are shown. The insets display the evolution of r_0 (in fm) with the number of iterations.

The three-body breakup $^6\mathrm{He} \rightarrow ^4\mathrm{He} + \mathrm{n} + \mathrm{n}$ was studied in [25], using a secondary ^{6}He ion beam of 240 MeV/N incident on carbon and lead targets. In particular, differential cross-sections $\mathrm{d}\sigma/\mathrm{d}E^*$ for inelastic excitations into the ^{6}He continuum (the $^4\mathrm{He} + \mathrm{n} + \mathrm{n}$ channel) were measured for both targets. The results showed that for a lead target the three-body breakup of ^{6}He was dominated by the electromagnetic dissociation. This fact allowed to extract the $E1$ strength function $\mathrm{d}B(E1)/\mathrm{d}E^*$ for ^{6}He, presented in fig. 4. This strength function is of great interest from the theoretical point of view, because the knowledge of this function simplifies essentially a comparison with calculations and it allows the use of cluster sum rules to extract information about the geometry of the ^{6}He ground-state wave function.

The experimental strength function in fig. 4 demonstrates clearly large $E1$ strength at low energies which leads to a very big electromagnetic cross-section in the order of 500 mb. The three-body calculations [39,40] shown in fig. 4, also predict a concentration of the strength at low energy. However, these calculations give $E1$ strength functions with maxima and more concentration at low energies than experimentally found. This fact has to be understood and some improvements in these calculations are needed. The non-energy-weighted $E1$ cluster sum rule reads $S_{\mathrm{clus}}^{\mathrm{NEW}} = \frac{3}{4\pi} Z_{\mathrm{c}}^2 e^2 \langle r_{\mathrm{c}}^2 \rangle$, where r_{c} is the distance between the core (the α-particle) and the center of mass of the whole ^{6}He nucleus. Using experimental $\mathrm{d}B(E1)/\mathrm{d}E^*$ shown in fig. 4 the root-mean-square distance $r_{\mathrm{c}} = 1.12 \pm 0.13$ (for ^{6}He) was obtained in [25]. This distance is in a good agreement with results obtained from three-body models [6] and it gives a complementary information about the structure of the ^{6}He halo nucleus.

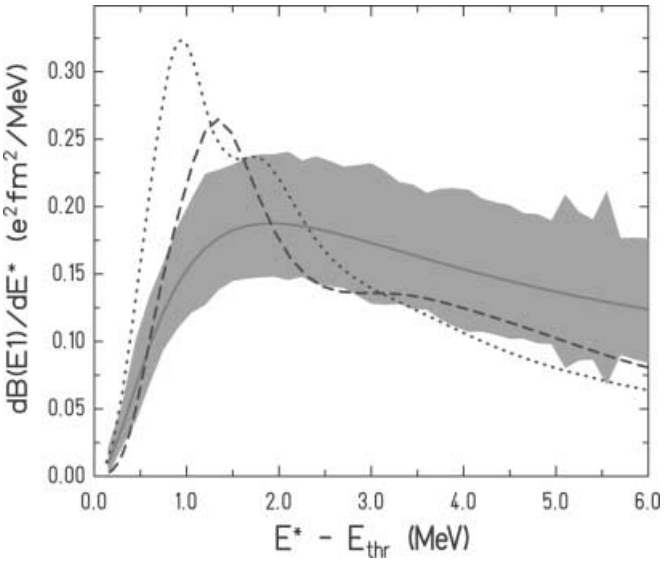

Fig. 4. The experimentally derived $E1$ strength distribution (for ^{6}He) and the errors are given by the solid line and the shaded band. Theoretical distributions are from [39] (dotted curve) and from [40] (dashed curve).

It should be mentioned that the ^{6}He halo nucleus is the theoretically most studied case among all Borromean nuclei. The reason for this is very simple and it is connected to fact that the binary α-n and n-n interactions are well known allowing three-body calculations practically without free parameters. The results of different three-body calculations for the ground state of ^{6}He generally agree with each other and demonstrate strong correlations in the ^{6}He ground-state wave function (see, for example, [6]). The correlation density plot for ^{6}He exhibits two prominent peaks (see, fig. 4 in [6]), a di-neutron peak with the two valence neutrons located close to each other and far from the α-particle core, and a cigar-like peak with the valence neutrons positioned on opposite sides of the α-particle. However, it is not a simple task to find experimental evidences for the existence of the di-neutron and cigar-like correlations in ^{6}He. One of the possibilities is to study the beta-decay of ^{6}He. A new branch of the ^{6}He beta-decay was found about 10 years ago [41]. In this paper the authors found the beta-delayed deuteron emission from ^{6}He. This decay seems to take place directly to the α-d continuum without going through resonance states in the daughter nucleus (^{6}Li). Subsequent theoretical studies [42,43] of this beta-decay, gave evidences that the di-neutron configuration in the ^{6}He ground-state wave function was mainly responsible for this process.

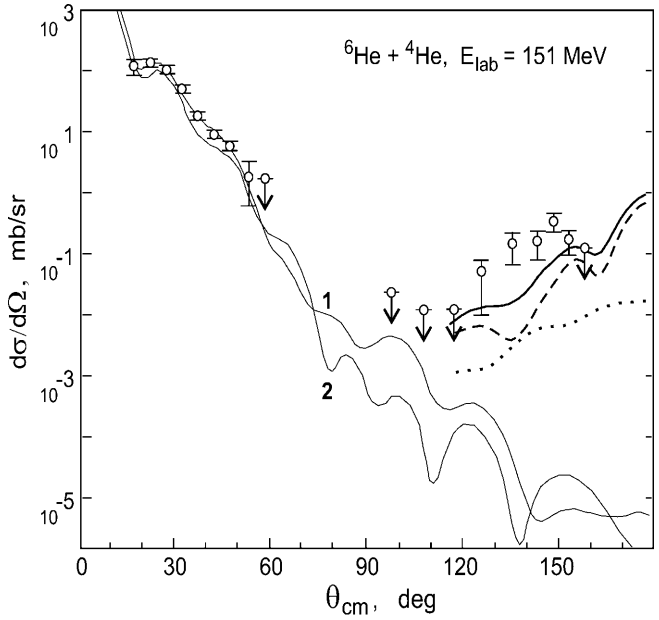

Fig. 5. ^{6}He + ^{4}He elastic scattering at $E_{\rm lab}$ = 151 MeV from [44]. The thin curves show the potential scattering. The thick solid line corresponds to the 2n exchange process, whereas the dashed and the dotted lines show the contributions of the di-neutron and cigar-like configurations of ^{6}He to the 2n-transfer process.

Recently the elastic scattering of ^{6}He + ^{4}He at the beam energy of 151 MeV has been measured [44]. Important peculiarity of this experiment is that elastic scattering cross-sections have been obtained in the broad center-of-mass angular region, including backward angles. These data are shown in fig. 5. One can see the increase of the cross-section at backward angles. Detailed theoretical treatment of the obtained data has been performed in [45]. It appears that at the backward angular range the experimental elastic scattering cross-sections is about 3 order of magnitude larger than that calculated with standard optical model code, shown by the thin curves in fig. 5. This comparison has lead the authors to the conclusion that the ^{6}He elastic-scattering events observed in the backward angular region are in fact the result of two-neutron exchange with the ^{4}He target nucleus. The calculated two-neutron transfer cross-sections, shown by the thick solid line in fig. 5, are in a good agreement with the experimental data. Moreover, the authors [45] have calculated separately the contributions of di-neutron and cigar-like configurations of ^{6}He to the two-neutron exchange (dashed and dotted lines in fig. 5). The contributions of the two components are quite different. At backward angles the di-neutron configuration of ^{6}He determines the two-neutron transfer reaction. One more important conclusion from these studies is that the three-body α-n-n configuration of the ^{6}He nucleus has a weight close to unity, *i.e.*, the spectroscopic factor $S_{(2n)\alpha}(^6\mathrm{He}) \approx 1$.

Experiments on three-body halo systems at high energies on light targets, where the core and one of the valence neutrons are detected, provide the opportunity to get the information about angular momentum structure of the halo. A correlation observable measured in such one-neutron knock-out (or stripping) reactions is the angular distribution of the relative momentum between two halo particles in the final state exhibited in a coordinate system with the z-axis along the center-of-mass momentum of the two-body system. This distribution is symmetric when either s^2 or p^2 states constitute the substructure in the three-body system. On the other hand, an equal mixture will produce a highly asymmetric distribution. Thus, this angular correlation highlights specific angular momentum properties of the initial three-body structure.

In a one-neutron stripping experiment with a 240 MeV/N ^{6}He ion beam [46] a large spin alignment of the ^{5}He fragment has been observed. The angular distribution of the $\mathbf{p}_{\alpha\text{-n}}$ vector relative to the direction of the $\mathbf{p}_{^5\mathrm{He}}$ is symmetric and shows an anisotropy, which can be described by a small admixture of the $(0p_{1/2})^2$ configuration [47] to the dominant $(0p_{3/2})^2$ configuration in the ^{6}He ground-state wave function. For ^{11}Li, a similar one-neutron stripping experiment [48] gives a skew angular distribution of the $\mathbf{p}_{^9\mathrm{Li\text{-}n}}$ vector relative to the direction of the $\mathbf{p}_{^{10}\mathrm{Li}}$. This is a model-independent way to demonstrate the mixing of s and p states in the ^{11}Li ground-state wave function, which has been, for rather long time, discussed in the literature (see, for example, [49]).

2.3 Borromean continuum

In contrast to the bound state the three-body continuum structure of Borromean nuclei is far from established and it is under active investigation now. Theoretical methods are available, but not systematically applied to halo nuclei. Note that the attractive potentials binding the three-body system are also able to produce resonances or at least non-uniform continuum structures. The difficulties are related to the spatial extension and the continuum structure of the subsystems being much more important for these excited structures.

Borromean continuum wave functions are solutions of the three-body (3→3) scattering problem. Thus, three-body dynamical equations should be solved with correct boundary conditions. For Borromean systems, where there is no binary bound state for any pair, there are true three-body asymptotics by Merkuriev [50] which are most naturally expressed via the rotational and permutational invariant hyperradius ρ [6] as $\rho^{-5/2}\exp(\pm k\rho)$ describing the out- and in-going three-body spherical waves.

Several few-body methods have been applied to search for resonances in ^{6}He: the hyperspherical harmonics method [40] where properties of the (3→3) scattering S matrix are investigated at real energies, the coordinate space Faddeev equations [39] with search for complex energy poles of the (3→3) scattering matrix, the complex scaling method [51], where the problem of resonant states is reduced to that of the bound states and the quantum Monte Carlo method [52], where the six-body problem has been solved with bound-state boundary conditions. The results of these investigations show that, except for

the known 0^+_1 and 2^+_1 states, one can expect additional three-body resonances 2^+_2,1^+ in the low-lying continuum of ^{6}He.

Very recently the results of investigations of the ^{6}Li(^{7}Li, ^{7}Be)^{6}He [53] and ^{6}Li(^{3}H, ^{3}He)^{6}He [54] charge exchange reactions, were reported. In both cases a broad structure in ^{6}He around $E_x \sim$ 4–5 MeV has been observed. The angular distributions of this structure show the dominance of a $\Delta L = 1$ transition, indicating the existence of low-lying dipole states in ^{6}He. It is important to note that in all calculations mentioned above, there were no clear evidence found for a soft dipole 1^- *resonance* at these excitation energies. More calculations and experiments are definitely needed to clarify this situation and to find a pronounced difference between the three-body continuum state and the three-body resonance.

3 Conclusion

In this paper we have discussed some examples of recent results obtained from experimental and theoretical studies of halo nuclei. We have concentrated on one- and two-neutron halos where few-body methods and techniques are very appropriate and play indispensable role in every adequate description of the discovered halo properties. The quantities discussed in the paper are chosen as the best illustrations of the dominating few-body features of structure and reactions. However, many other properties, related to two- and three-body halos, have been studied over the last decade, which we have not discussed in this paper and which are making the whole picture of halo nuclei essentially richer.

References

1. A. Navin *et al.*, Phys. Rev. Lett. **85**, 266 (2000).
2. I. Iwasaki *et al.*, Phys. Lett. B **481**, 7 (2000).
3. A. Ozawa *et al.*, Phys. Rev. Lett. **84**, 5493 (2000).
4. I. Tanihata *et al.*, Phys. Rev. Lett. **55**, 2676 (1985).
5. P.G. Hansen, B. Jonson, Europhys. Lett. **4**, 409 (1987).
6. M.V. Zhukov *et al.*, Phys. Rep. **231**, 151 (1993).
7. P.G. Hansen, A.S. Jensen, B. Jonson, Annu. Rev. Nucl. Part. Sci. **45**, 591 (1995).
8. I. Tanihata, J. Phys. G **22**, 157 (1996).
9. M.H. Smedberg *et al.*, Phys. Lett. B **452**, 1 (1999).
10. L.V. Grigorenko *et al.*, Phys. Rev. C **60**, 044312 (1999).
11. M.V. Zhukov, I.J. Thompson, Phys. Rev. C **52**, 3505 (1995).
12. J.S. Al-Khalili, J.A. Tolstevin, Phys. Rev. Lett. **76**, 3903 (1996).
13. L.V. Chulkov *et al.*, Europhys. Lett. **8**, 245 (1989).
14. K. Riisager, A.S. Jensen, P. Møller, Nucl. Phys. A **548**, 393 (1992).
15. T. Nakamura *et al.*, Phys. Rev. Lett. **83**, 1112 (1999).
16. S. Fortier *et al.*, Phys. Lett. B **461**, 22 (1999).
17. W. Geithner *et al.*, Phys. Rev. Lett. **83**, 3792 (2000).
18. F.M. Nunes, I.J. Thompson, R.C. Jonhson, Nucl. Phys. A **596**, 171 (1996).
19. D. Ridikas *et al.*, Nucl. Phys. A **628**, 363 (1998).
20. T. Aumann *et al.*, Phys. Rev. Lett. **84**, 35 (2000).
21. J.A. Tostevin, J. Phys. G **25**, 735 (1999).
22. Yu.L. Parfenova, M.V. Zhukov, J.S. Vaagen, Phys. Rev. C **62**, 044602 (2000).
23. D. Bazin *et al.*, Phys. Rev. C **57**, 2156 (1998).
24. A. Navin *et al.*, *Proceedings of Experimental Nuclear Physics in Europe (ENPE 99), Sevilla 1999*, edited by B. Rubio *et al.*, AIP Conf. Proc. Vol. **495** (AIP, New York, 1999) p. 309.
25. T. Aumann *et al.*, Phys. Rev. C **59**, 1252 (1999).
26. M. Zinger *et al.*, Nucl. Phys. A **619**, 151 (1997).
27. M.V. Zhukov, B. Jonson, Nucl. Phys. A **589**, 1 (1995).
28. H. Esbensen, Phys. Rev. C **53**, 2007 (1996).
29. P.G. Hansen, Phys. Rev. Lett. **77**, 1016 (1997).
30. F. Barranko, E. Vigezzi, R.A. Broglia, Phys. Lett. B **319**, 387 (1993).
31. A.A. Korsheninnikov, T. Kobayashi, Nucl. Phys. A **567**, 97 (1994).
32. S.N. Ershov *et al.*, Phys. Rev. Lett. **82**, 908 (1999).
33. Y. Suzuki *et al.*, Nucl. Phys. A **567**, 957 (1994).
34. G.F. Bertsch, K. Henken, H. Esbensen, Phys. Rev. C **57**, 1366 (1998).
35. E. Garrido, D.V. Fedorov, A.S. Jensen, Phys. Lett. B **480**, 32 (2000).
36. S.N. Ershov, B.V. Danilin, J.S. Vaagen, Phys. Rev. C **62**, 041001(R) (2000).
37. F.M. Marques *et al.*, Phys. Lett. B **476**, 219 (2000).
38. I.J. Thompson, M.V. Zhukov, Phys. Rev. C **53**, 708 (1996).
39. A. Cobis, D.V. Fedorov, A.S. Jensen, Phys. Rev. C **58**, 1403 (1998).
40. B.V. Danilin *et al.*, Nucl. Phys. A **632**, 383 (1998).
41. K. Riisager *et al.*, Phys. Lett. B **235**, 30 (1990).
42. M.V. Zhukov *et al.*, Phys. Rev. C **47**, 2937 (1993).
43. D. Baye *et al.*, Prog. Theor. Phys. **91**, 271 (1994).
44. G.M. Ter-Akopian *et al.*, Phys. Lett. B **426**, 251 (1998).
45. Yu.Ts. Oganessian, V.I. Zagrebaev, J.S. Vaagen, Phys. Rev. Lett. **82**, 4996 (1999).
46. L.V. Chulkov *et al.*, Phys. Rev. Lett. **79**, 201 (1997).
47. L.V. Chulkov, G. Schrieder, Z. Phys. A **359**, 231 (1997).
48. H. Simon *et al.*, Phys. Rev. Lett. **83**, 496 (1999).
49. I.J. Thompson, M.V. Zhukov, Phys. Rev. C **47**, 1904 (1994).
50. S.P. Merkuriev, Sov. J. Nucl. Phys. **19**, 447 (1974).
51. S. Aoyama *et al.*, Prog. Theor. Phys. **93**, 99 (1995); **94**, 343 (1995)
52. R.B. Wiringa *et al.*, Phys. Rev. C **62**, 014001 (2000).
53. S. Nakayama *et al.*, Phys. Rev. Lett. **85**, 262 (2000).
54. T. Nakamura *et al.*, Phys. Lett. B **493**, 209 (2000).